Oral Presentation

The 7th TSME International Conference on Mechanical Engineering
13-16 December 2016

TSME ICOME 2016
Mechanical Engineering Innovation for Green Society

MSN0003

Influence of Scratch Marks on Undeformed Chip Thickness with a Straight Diamond Tool

Keisuke Amaki[1, *], Yukio Maeda[1], Tomohiro Iida[1], Kazuya Kato[2], Hideki Tanaka[2], Takanori Yazawa[3], and Tatsuki Otsubo[4]

[1] Toyama Prefectural University, 5180 Kurokawa, Imizu-shi, Toyama, 939-0398, Japan
[2]Shonan Institute of Technology, 1-1-25 Tsujido-nishikaigan, Fujisawa-shi, Kanagawa, 251-0046, Japan
[3]Nagasaki University, 1-14 Bunkyo-machi, Nagasaki-shi, Nagasaki, 852-8521, Japan
[4]Salesian Polytechnic, 4-6-8 Oyamagaoka, Matida-shi, Tokyo, 194-0215, Japan
[*]Keisuke Amaki:keisuke.amaki.29@gmail.com, +81-766-56-7500, +81-766-56-8030

Abstract

Recently, high efficiency and high performance have become to be required of information equipment, such as laser printers. As a result, optical scanning parts that reduce optical aberration, scatter, and diffraction are required in laser printers. Polygon mirrors are manufactured by polishing a plating or glassy material to a mirror finish. In this study, we shorten the manufacturing process to improve the productivity and ultra-precision cutting technology of polygon mirrors made of Al-Mg alloys. Therefore, it is necessary to improve the geometric surface roughness achieved during the mirror cutting of Al-Mg alloys and to remove tear-out marks and scratch marks that occur during the cutting process. We investigated the cutting edge shape using a straight diamond tool to decrease surface defects during ultra-precision cutting of Al-Mg alloys. We found that the scratch marks caused by crystallization which was crashed at tool produce small pieces, then the small pieces caused scratch marks. We improved the cutting edge shape by using a straight diamond tool to remove scratch marks and we investigated the influence of surface defects. As a result, we clarified that ductility mode processing of the crystallization was possible by the undeformed chip thickness of less than 100 nm.

Keywords*:* Ultra-precision cutting, Al-Mg alloys, Diamond tool, Scratch marks, Undeformed chip thickness

1. Introduction

Recently, increasingly high efficiency and high performance have become essential requirements of information equipment such as the laser printers shown in Fig. 1 [1, 2]. As a result, optical scanning parts that reduce optical aberration, scatter, and diffraction are now required in laser printers [3, 4]. Figure 2 shows examples of microphotographs and surface roughness profiles of machined surfaces [5]. In this study, we shorten the manufacturing process to improve the productivity and ultra-precision cutting technology of polygon mirrors made of aluminium alloys. It is necessary to improve the geometric surface roughness achieved in the mirror cutting of Al-Mg alloys [6, 7] and remove tear-out marks and scratch marks that occur during the cutting process [8]. Therefore, we investigated the cutting edge shape using a diamond tool to decrease scratch marks in the ultra-precision cutting of Al-Mg alloys.

2. Experimental Results and Considerations

The cutting conditions are summarized in Table 1, and the experimental setup is shown in Fig. 3. Machined surface damage due to entwining chips was restrained using the minimum quantity of lubrication (MQL) required and a chip collector. Machined surface damage due to entwining chips was restricted using the minimum quantity of lubrication (MQL) required and a chip collector.

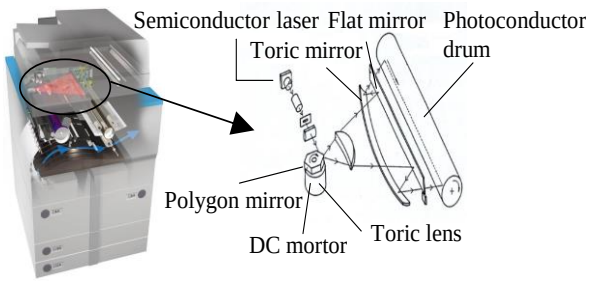

Fig. 1 Optical parts of a laser printer

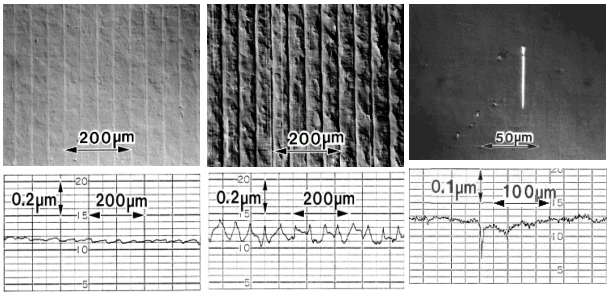

(a) Geometrical surface roughness (b) Tear-out marks (c) Scratch marks

Fig. 2 Photographs and surface roughness profiles of machined surfaces

MSN0003

3. Results from Prior Experimentation

3.1 Straight tool

Figure 4 shows the surface generation model for a straight tool. With a positive tool setting angle, the surface roughness increases because tear-out marks occur on the side cutting edge. With a negative tool setting angle, we achieve a good machined surface without tear-out marks. The reason for this is that the tear-out marks are removed by the end cutting edge. However, these methods cannot support a high feed rate, since wear is a time-consuming process. A straight tool has been used to produce a good machined surface without tear-out marks only in a narrow range of tool setting angles, which range from −0.015° to −0.008° [9-11].

3.2 Double-facet tool

We produced a double-facet tool to expand the range of the tool setting angle. Figure 5 shows the cutting edge shape of the double-facet tool and Fig. 6 shows the surface generation model for a double-facet tool. In addition, it is difficult to give a direct micro facet. Therefore, we produced a double-facet tool that has a side rake angle on the rake face to produce a pseudo-facet. The use of the double-facet tool results in a 10 fold increase in the range of the tool setting angle. This will produce a good machined surface without tear-out marks. However, when the feed rate was over 100 μm/rev, there were tear-out marks and scratch marks on the processing face.

4. Mechanism of Scratch Mark Formations

The use of a double-facet tool cannot remove scratch marks. Therefore, we investigated the scratch mark formations. We observed the scratch marks using a differential interference microscope. As an example of the processing, Fig. 7 shows photographs of these scratch marks. We observed the processing face prior to cutting and discovered crystallization. We observed crystallization by means of Scanning Electron Microscopy (SEM), and the cross-section is shown in Fig. 8. In addition, we analyzed the elements of crystallization using Energy Dispersive X-ray spectrometry (EDX). The ingredient analysis of the crystallization is shown in Fig. 9. The results, show that the crystallization includes Al, Mg, Si, M and Fe [20]. Therefore, we know that it was formed by hard crystallization, e.g., an inclusion of Al-Fe-Si, though EDX analysis. Figure 10 shows the cross-section profiles of the scratch marks. Figure 10 (a) shows the cross-section prior to cut the crystallization. The result shows that there was a bump of 2 μm at the starting point of the scratch marks. Figure 10 (b) shows the cross-section after cutting the crystallization. We found that there was a 0.6 μm groove in the section. We investigated the relationship between the shape of the scratch marks and the number of the scratch marks laps. The relationship between the shape and number of laps is shown in Fig. 11. This figure shows that the depth of the scratch mark increases as the number of

Table. 1 Experimental equipment and conditions

Machine tool	NC ultra-precision turning machine ULG100C
Cutting tool	Diamond tool (single crystal diamond)
Work piece	A5186 OD 130 mm × ID 40 mm
Cutting conditions	Cutting speed: V = 193 ～ 628 m/min Feed rate: F = 50 ~ 200 μm/rev Depth of cut: t = 30 μm Tool setting angle θ: −0.5° ~ 0.5°
Lubricating system	MQL
Cutting fluid	UP-2A
Chip collector	GSB-10537exP
Dynamometer	Type9251A KISTLER

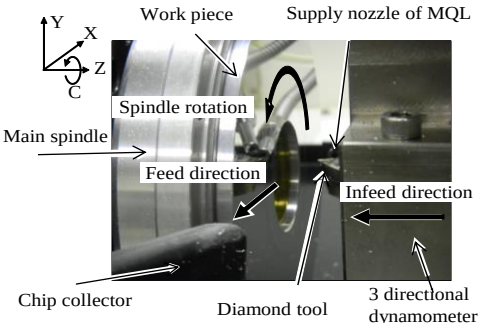

Fig. 3 Setup of experiment

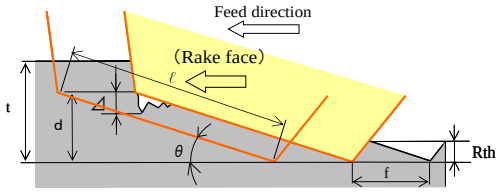

Fig. 4 Surface generation model using a straight tool

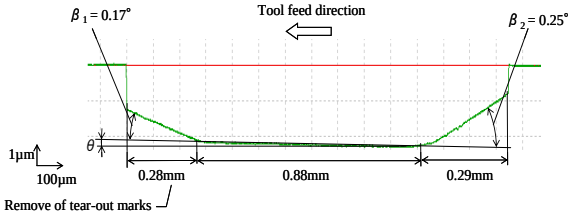

Fig. 5 The cutting edge shape of a double-facet tool

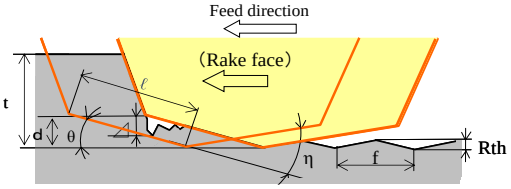

Fig. 6 Surface generation model using a double-facet tool

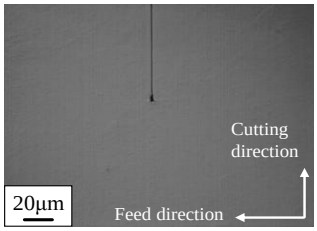

Fig. 7 Photograph of the scratch marks taken from the differential interference microscope

laps of scratch marks increases. Similarly, the width of the scratch mark increases with the number of laps. As a result, we concluded that the scratch marks were formed as a result of crystallization. The mechanism of scratch formation is shown in Fig. 12. We found that the tool crashed against the bumps formed by crystallization, producing small pieces. Then, these pieces attached to the end cutting edge and acted as micro cutting edges. As a result, these small pieces caused the scratch marks. Therefore, we expect that the ductility-mode processing of an inclusion is possible if the depth of the cut is small.

5. Cutting Characteristic of the Triple-Facet Tool

Based on the mechanism of scratch mark generation, the ductility-mode processing of an inclusion can be expected if the depth of the cut is small. We developed a triple-facet tool with a double-facet at the end cutting edge to remove scratch marks and investigated the influence of surface defects. We show the cutting edge shape of a triple-facet tool in Fig. 13. This tool has two micro facets at the end cutting edge and can perform micro cutting. In addition, micro-facet β_2 removes tear-out marks, and micro-facet β_1 removes scratch marks. The removal of tear-out marks and scratch marks separately by each micro-facet produces a good machined surface.

5.1 Reduction in surface defects by using triple-facet tool

We varied the tool setting angle θ, and analyzed the influence of the triple-facet tool on the surface characteristics. The relationship between tool setting angle and surface roughness is shown in Fig. 14. The feed rate f was 50 μm/rev in this experiment. Figuer14 shows that the use of the triple-facet tool at a tool setting angle of -0.1° to 0.1° results in a good machined surface roughness. We calculated theoretical surface roughness Hth of the triple-facet tool with Eq. 1. In addition, in the tool setting angle range of 0° to 0.05°, we achieved a good machined surface without tear-out and scratch marks. Next, we investigated the relationship between the scratch marks and the undeformed chip thickness.

$$\mathrm{Hth} = \frac{f}{\cot(\beta_3 - \theta_3) + \cot\theta}, \quad (-0.065° < \theta_3 < 0°)$$

$$\mathrm{Hth} = \frac{f}{\cot\theta_1 + \cot(\beta_1 - \theta_1)}, \quad (0° < \theta_1 < 0.07°)$$

$$\mathrm{Hth} = \frac{f}{\cot(\beta_2 - \theta_2) + \cot(\theta_2 - \beta_1)}. \quad (1)$$

$$(0.07° < \theta_2 < 0.16°)$$

5.2 Influence of scratch marks on undeformed chip thickness for triple-facet tool

Figure 15 shows the relationship between the tool setting angle and the undeformed chip thickness with a triple-facet tool when the feed rate is 50 μm/rev. We calculated the undeformed chip thickness n of the

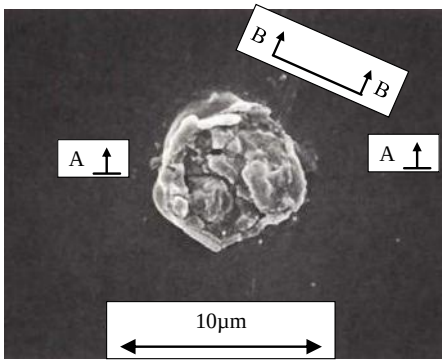

Fig. 8 Photograph of the crystallization with the shape measuring SEM.

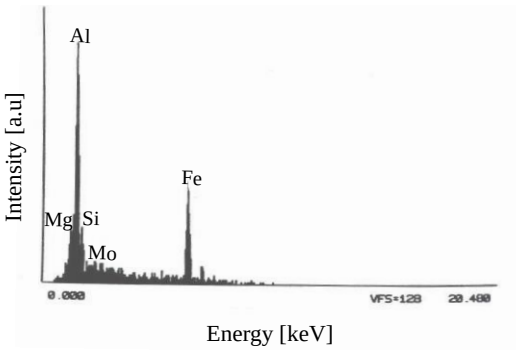

Fig. 9 Ingredient analysis of the crystallization

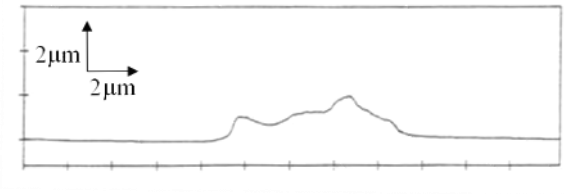

(a) Cross-section of the scratch marks (A-A)

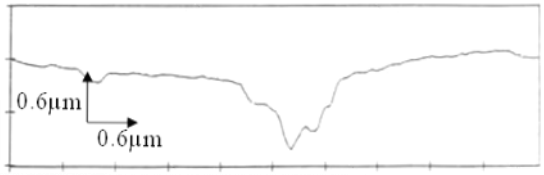

(b) Cross-section of the scratch marks (B-B)

Fig. 10 Cross-sectional profile of scratch marks

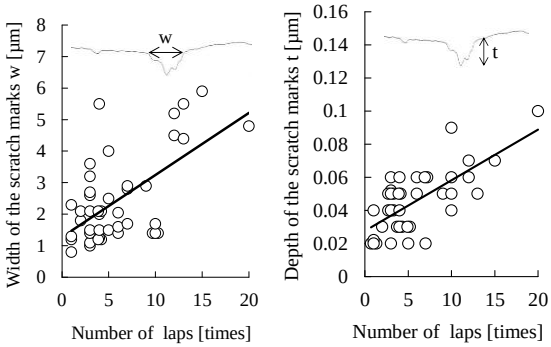

Fig. 11 Relationship between the shape and the number of laps

triple-facet tool with Eq. 2. When the tool setting angle is between 0° and 0.05°, scratch marks are removed. We can achieve good machined surface roughness without scratch marks when the undeformed chip thickness is less than 60 nm. Therefore, the use of the triple-facet tool is possible the ductility mode processing of a crystsllization. However, when the feed rate was over 100 μm/rev, there were tear-out marks and scratch marks on the machined face.

$$n = f \times \sin(\beta_1 - \theta_1) \quad (0° \leqq \theta_1 < 0.07°),$$

$$n = f \times \sin(\beta_2 - \theta_2) \quad (0.07° \leqq \theta_2 < 0.14°). \qquad (2)$$

6. Cutting Characteristic of the Improved Triple-Facet Tool

The triple-facet tool caused tear-out marks and scratch marks on the machined surface if the feed rate was over 100 μm/rev. We thought that the tool had not functioned well enough to cut because the cutting edge length, which reduces scratch marks, was short. Therefore, we improved the cutting edge length by increasing it to 400μm from 160μm. We show the cutting edge shape of an improved triple-facet tool in Fig.16. We investigated the influence of surface defects when the feed rate is 100 to 200 μm/rev. However, a machined surface roughness better than the theoretical surface roughness was achieved. Therefore, we observed the cutting edge shape of an improved triple-facet tool in detail. Figure 17 shows an enlarged view of the end cutting edge and micro facet β_1. A dashed line is the ideal cutting edge shape. As can be seen from the Fig.17, there was a round part on the end cutting edge and micro facet β_1. We expressed that round part as a red line. We defined the cutting edge with length of 580 μm as the end cutting edge and angle of the end cutting edge for machined surface as θ'. In addition, we defined β_0 and β_1 as the angles of each cutting edge for the end cutting edge. The experimental results showed that we achieved a good machined surface without tear-out or scratch marks in the range of the tool setting angle, θ', from 0.01° to 0.05°. Also, the feed rate was 100 and 150 μm/rev. Next, we investigated the influence of surface defects when the feed rate is 200 μm/rev. Figure 18 shows the relationship between the tool setting angle, θ', and the surface roughness when the feed rate is 200 μm/rev. We calculated the theoretical surface roughness, Hth, of the improved triple-facet tool with Eq. 3. This figure shows that we achieved a good machined surface roughness with a tool setting angle range of 0.01° to 0.05°. In addition, when the tool setting angle is 0.04° and 0.05°, there were tear-out marks on the machined surface. When the tool setting angle is 0.01° to 0.03°, we can produce a good machined surface without tear-out and scratch marks. Therefore, we investigated the influence of scratch marks on undeformed chip thickness for improved triple-facet tool.

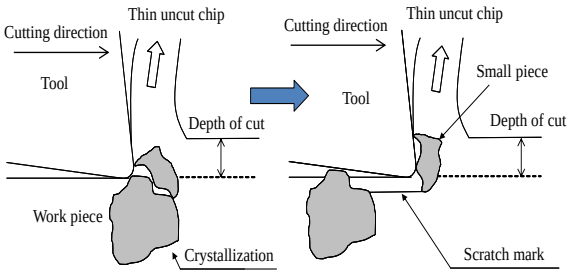

Fig. 12 Schematic of scratch mark formation

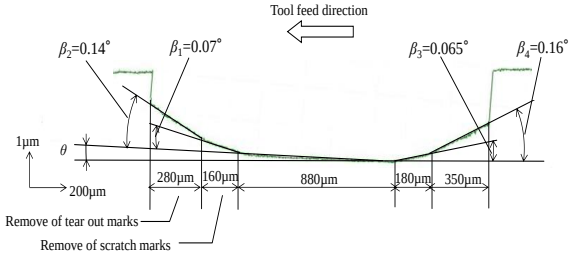

Fig. 13 Cutting edge shape of the triple-facet tool

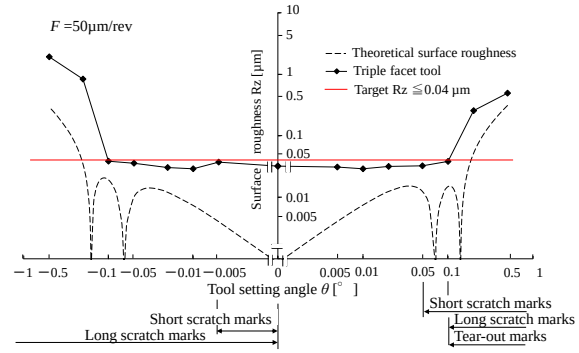

Fig. 14 Relationship between tool setting angle and surface roughness with the triple-facet tool

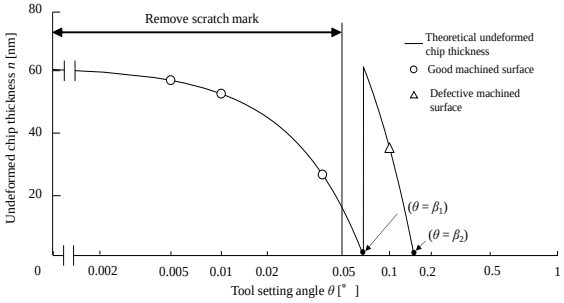

Fig.15 Relationship between tool setting angle and umdeformed chip thickness with the triple-facet tool

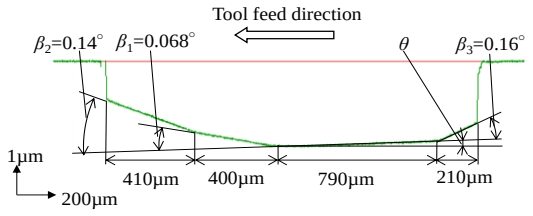

Fig.16 Cutting edge shape of improved triple-facet tool

MSN0003

$$Hth = \frac{f}{\cot(\beta_0 - \theta_1') + \cot\theta_1'}, \quad (0° < \theta_1' < 0.036°)$$

$$Hth = \frac{f}{\cot(\beta_1 - \theta_2') + \cot(\theta_2' - \beta_0)}.$$

$$(0.036° < \theta_2' < 0.081°) \qquad (3)$$

7. Influence of Scratch Marks on Undeformed Chip Thickness

The presence of scratch marks on a machined surface depends on the sharpness of the diamond tool's cutting edge and machining condition. Figure 19 shows the relationship between the tool setting angle and the undeformed chip thickness for each tool. We calculated the undeformed chip thickness, *n*, of the improved triple-facet tool with Eq. 4. This figure shows that we achieved a good machined surface roughness without scratch marks when the undeformed chip thickness is less than 100 nm. The use of the improved triple-facet tool enable the cutting in feed rate 200μm/rev. The feed rate is 4 fold as much high efficiency as 50μm/rev in the double-facet tool and the triple-facet tool.

$$n = f \times \sin(\beta_1 - \theta_1'), \ (0° \leqq \theta_1' < 0.068°)$$
$$n = f \times \sin(\beta_2 - \theta_2'). \ (0.068° \leqq \theta_2' < 0.14°) \qquad (4)$$

It is confirmed that there is ductility mode cutting when the undeformed chip thickness is smaller than the radius of the tool's cutting edge [12-14]. Therefore, we measured the cutting edge radius of the double-facet tool, the triple-facet tool, and the improved triple-facet tool. Figures 20 – 22 shows the cutting edge radius of the double-facet tool, the triple-facet tool, and the improved triple-facet tool. We measured the radiuses using Scanning Electron Microscopy (SEM) of ELIONIX. The results showed that the radius of the cutting edges for the double-facet, triple-facet, and improved triple-facet tools were 108 nm, 120 nm, and 115 nm, respectively. The cutting edge radius of the improved triple-facet tool is larger than the undeformed chip thickness shown in Fig. 19. So, it is assumed that the use of the improved triple-facet tool achieved good machined surface roughness without scratch marks when the undeformed chip thickness is less than 100 nm.

8. Conclusions

This study investigated the influence of scratch marks on undeformed chip thickness with a straight diamond tool. The following results were obtained:

(1) Mechanism of scratch mark formation

The starting point of scratch is a hard crystallization. The tool crashed against the bumps formed by crystallization, producing small pieces, and then, these small pieces caused scratch marks.

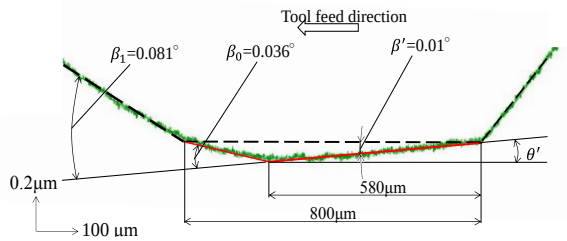

Fig. 17 Enlarged view of the cutting edge shape

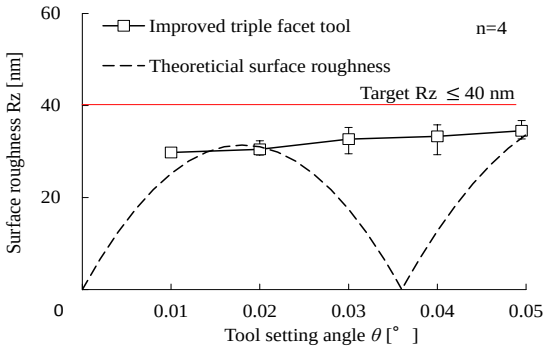

Fig.18 Relationship between tool setting angle and surface roughness with the improved triple-facet tool

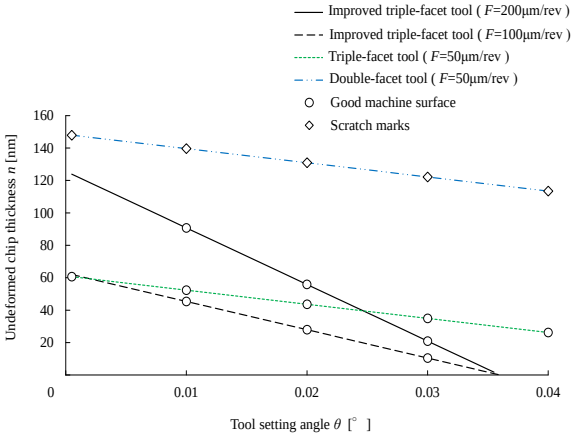

Fig.19 Relationship between tool setting angle and umdeformed chip thickness with the improved triple-facet tool

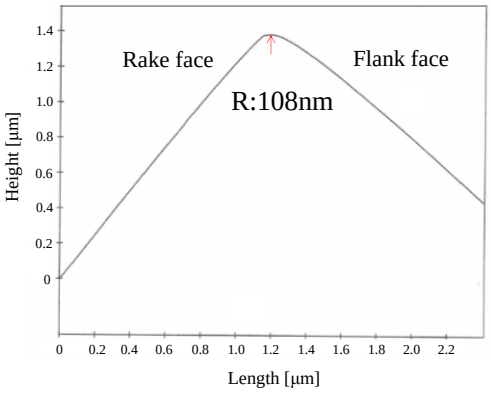

Fig. 20 The tool cutting edge radius of the double-facet tool

(2) Examination about reduce scratch marks

The use of the improved triple-facet tool can achieve good machined surface roughness Rz ≦ 40nm without scratch marks when the undeformed chip thickness is less than 100 nm.

8. References

[1] Kawamura, A. Suzuki, S. and Hayashi, Y. (2003). Hand of Laser Technology and Applications, CRC press, pp. 2421- 2462.

[2] Matuda, T. Mikami, T. and Abe, F. (1983). The correction method of the optical beam scanning error of a rotation polygon mirror, Journal of the Institute of Electronics, Information and Communication Engineers, vol.J6−C, No.2, pp137−144. (in Japanese)

[3] Kato, Y. Umeda, H. and Hoshino, K. (2005). Alminum ally substrate for high density magnetic memory disks, Kobe steel engineering reports, vol. 55, No.2.

[4] Whiteen, L. G. and Lewis, T. G. (1983). Machining and mesurment to submicron tolerances, Proc. M.T.D.R, pp-491.

[5] Maeda, Y. Masami, M. Nishiguchi, T. Sawa, M. and Ito, R. (1986). A Study on Diamond Turning of Al−Mg Alloy Generation Mechanism of Surface Machined with Worn Tool, Annals of the CIRP, vol.38-1, pp.111-114.

[6] Teaching materials development committee. (1991). Ultra-precision cutting of the polygonmirror, Magazine of occupation development report, pp-9-10. (in Japanese)

[7] Tanaka, K. (1987). Development of polygon mirror generator, Journal of japan society for presision engineering, vol.53, No.6, pp-23-24. (in Japanese)

[8] Ou, H. Maeda, Y. Sinji, S. Nisiguchi, T. and Masuda, M. (2000). Reduction of tear-out marks in diamond cutting of alluminum alloys, High processiing, vol.19, pp42-48. (in Japanese)

[9] Maeda, Y. (1991). Sutudy on processing precision inorivement in ultra-precision cutting, Dictoral dissertation, pp-27-29.

[10] Sawa, M. Maeda, Y. and Masami, M. (1993). Development of an advanced tool-setting device for diamond turning, annals of the CIRP, Vol.42, pp87-90.

[11] Iida, T. Maeda, Y. Hirase, D. Motoyoshi, T. Tanaka, H. Kato, K. and Yazawa, T. (2015). Influence of tool shape on cutting characteristics in ultra-precision cutting of Al-Mg alloys, Advanced Materials Research, Vol. 806, November 2015, pp. 178-183.

[12] P.Li, X. He, T. Rahman, M. (2005). Tool Wear Characteristics and Their Effects on Nanoscale Ductile Mode cutting of Silicon Wafer. vol.259, July – August 2005, pp. 1207 – 1214.

[13] Cai, M.B. Li, X.P. Rahman, M. Tay, A.A.O. (2007). Crack initiation in Relation to the Tool Edge Radius and Cutting Conditions in Nanoscale Cutting of Silicon. vol.47, March 2007, pp. 562 – 569.

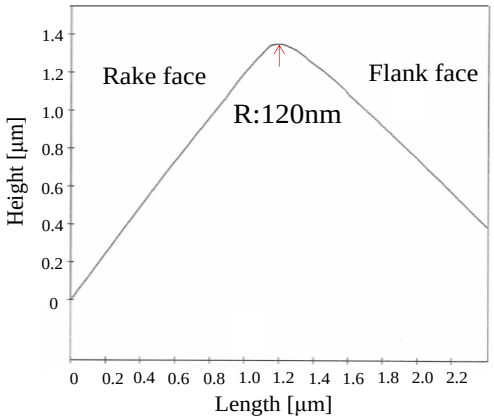

Fig. 21 The tool cutting edge radius of the triple-facet tool

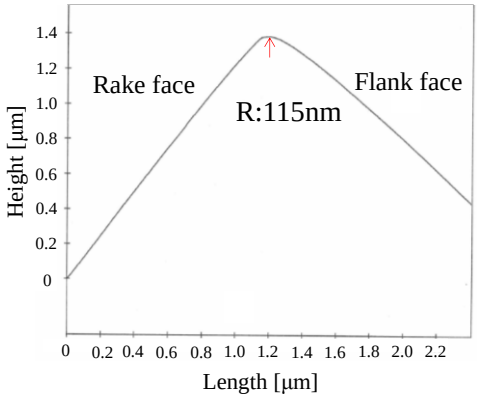

Fig. 22 The tool cutting edge radius of the improved triple-facet tool

[14] Cai, M.B. Li, X.P. Rahman, M. (2007). Study of the Mechanism of Nanoscale Ductile Mode Cutting of Silicon Using Molecular Dynamics Simulation. vol.47, January 2007, pp. 75 – 80.